Analog Integrated Circuits and Signal Processing (2019) 101:659–668
https://doi.org/10.1007/s10470-019-01549-0

Optimization and development of the RF MEMS structures for low voltage, high isolation and low stress

Hamid Reza Ansari[1] · Mojtaba Behnam Taghaddosi[1]

Received: 22 June 2019 / Revised: 22 June 2019 / Accepted: 3 October 2019 / Published online: 12 October 2019
© Springer Science+Business Media, LLC, part of Springer Nature 2019

Abstract

MEMS capacitive switches have longer lifetimes compared to other types of metal-to-metal switches, and when placed on the membrane on the transmission line, they can easily return to the up-state due to a dielectric layer. They also transmit the input signal with more power and frequency and therefore, they are better than metal-to-metal switches. In this paper, first three switches were considered as the basic structures. Then, in order to demonstrate the credibility and high quality of the simulations, the same switches were simulated. The obtained results are very close to the results of fabrication of these switches. In the next step, with the presentation of three new structures, stimulation voltage, stress, switching time and isolation were improved in four steps. The mechanical simulation of the switch was performed to determine the amount of displacement, the amount of stress and the resonant frequency using the COMSOL software. In addition, electrical simulation of the switch was performed to obtain the S-parameter using the HFSS software. The simulation results demonstrate that the isolation is 57–66 dB and the insertion loss is 0.3–2 dB in the desired frequency band (1–50 GHz). Using new spring structures, the actuation voltage was reduced from 4.8 V in basic structures (the smallest in three structures) to 2.4 V in new structures, which is considered excellent. In order to increase the lifetime of the switch, the stress in the new switches is reduced from 12 to 4.5 MPa compared to the basic switches.

Keywords RF MEMS switch · Low actuation voltage · High isolation · Low stress

1 Introduction

Radio frequency micro-electromechanical switches (RF MEMS) have a much better performance at high frequencies compared to similar ones, including FET switches and p-i-n diode switches. The advantages of these switches include low power consumption, high cut-off frequency, high electrical isolation in all frequency bands, small size and low weight [1, 2]. MEMS switches can be divided into several types based on the type of actuation (electrostatic, electromagnetic, electrothermal and piezoelectric), circuit configuration (series or parallel), and the type of connection to the transmission line (capacitor or metal-to-metal). Discussion on these cases and the choice of an optimal switch was done in [3, 4].

One of the disadvantages of RF MEMS switches is the high actuation voltage, low power transmission and high stress on the beam after the switch actuation. Each of these can significantly reduce the lifetime of the switch. In recent years, many works have been done to eliminate the actuation voltage problem, including increasing the cross-section, reducing the hardness of the spring and reducing the initial gap [5]. In addition, to reduce the amount of stress applied to the beam after the actuating of the switch, one can use the step structure in the beam and the two-height spring with elasticity in the vertical direction [6].

RF MEMS switches have been extensively used in space and military industries due to low power consumption losses of almost zero over the past two decades, and therefore improving the performance of these switches is considered very important. Furthermore, these systems are very suitable for use in radar, cell phone, Bluetooth and

✉ Mojtaba Behnam Taghaddosi
mjtbbehnam121@gmail.com

Hamid Reza Ansari
hr.ansari@imamreza.ac.ir

[1] Electrical Engineering Department, Imam Reza International University, Mashhad, Iran

Wi-Fi applications in the frequency range of 30 kHz–300 GHz [3, 4, 7].

Following the improvements made to micro-electromechanical systems over the past twenty years, switches with the excellent characteristics and parameters in recent years are simulated. The results of some of the simulation of these switches are as follows:

In [8], three structures with low spring coefficients were proposed to reduce the actuation voltage of the switch. These switches are used in circuits in series. The actuation voltage for these structures varies between 6 and 14 volts, and the good RF specifications include an isolation of − 70 dB to − 76 dB and an insertion loss between 0.005 and 0.06 dB at a frequency of 10 GHz. A capacitive RF MEMS switch was fabricated using two high-impedance transmission lines in [9]. One of the advantages of this switch is to eliminate the surface roughness by presenting a new manufacturing method, which results in a good S-parameter. For this switch, the actuation voltage is equal to 20 V. In addition, the results obtained after RF analysis demonstrate better isolation than 18 dB and return loss less than − 20 dB in the C-K band. Given that in the manufacture of MEMS switches, the stiffness coefficient is usually higher than 10 N/m, but the three switches fabricated in [10] have a stiffness coefficient of 1.34–1.56 N/m. This reduction in the spring-stiffness coefficient leads to a decrease in the actuation voltage of about 4.8–6.3 V. In addition, for these three structures, the best isolation was 40 dB at 17 GHz and the best insertion loss was 0.25 dB at 20 GHz. A single membrane switch with a 4.3 V actuation voltage was fabricated in [11]. This switch has good RF characteristics, including a 36 dB isolation and an insertion loss of 0.52–2.05 dB at a frequency of 20 GHz.

In this paper, at first three switches fabricated in [10] are exactly simulated and then, the results of this simulation are compared with the results of the fabrication. The purpose of this comparison is to demonstrate the high quality and credibility of simulations. Then, some of the parameters of the three basic switches are optimized in four steps. These parameters included stress, switching time, actuation voltage, and isolation.

2 The common structure of an RF MEMS switch

In RF MEMS switches a microstrip line or Coplanar Waveguide (CPW) line on the substrate are typically use, which is preferable to microstrip due to easier access to ground plates. Capacitive switches are often used in circuits with parallel configurations. The difference in parallel and series configuration is in capacitor coupling in determining the operating frequency of the switch. In the parallel configuration, the switch has the ability to function up to 200 GHz, while in the series configuration this ability reduces to 20 GHz. Another advantage of capacitive switches is the insertion of a dielectric layer between the beam and the transmission line, which prevents the switch from direct contact with the membrane and the transmission line and increases the lifetime of the switch in the high number of cycles. The schematic diagram of the MEMS capacitive switch in up and down states is shown in Fig. 1a and Fig. 1b, respectively. As shown in Fig. 1b, after applying the voltage to the beam, the RF input and output are connected to each other and the switch is in the on state. To obtain the voltage required to actuate this switch, one can use Eq. 1:

$$V_{pull-in} = \sqrt{\frac{8k_T g_i^3}{27\varepsilon_0 A}} \quad (1)$$

where $V_{pull-in}$ is the actuation voltage, g_i the initial gap between the beam and the dielectric, ε_0 the permeation coefficient of the vacuum and A the cross-sectional of the overlap area. It should be noted that for the design of a MEMS switch, the transmission line impedance must be equal to 50 Ω. The impedance of the transmission line depends on the substrate and switch type, the gap between the transmission line and the ground, the width of the transmission line and the height of the substrate. The electrical model of an RF MEMS capacitive switch is illustrated in Fig. 1c.

One of the most effective parameters to improve the RF performance is the high capacitive ratio, which requires a maximum capacitor in the down state and a minimum capacitor in the up state. Equations 2 and 3 can be used to obtain the down state and up state capacitors, respectively. As seen in these Equations, the gap change will lead to fundamental changes in the value of the up state capacitor. In addition, the capacitance ratio of the switch can be calculated using Eq. 4. By increasing the capacitive ratio of the switch, excellent RF performance can be achieved, resulting in high isolation and low losses.

$$C_{down} = \frac{\varepsilon_0 \varepsilon_r A}{t_d} \quad (2)$$

$$C_{up} = \frac{\varepsilon_0 A}{g_i + \frac{t_d}{\varepsilon_r}} \quad (3)$$

$$\mathrm{CR} = \frac{C_{down}}{C_{up}} = \frac{\frac{\varepsilon_0 \varepsilon_r A}{t_d}}{\frac{\varepsilon_0 A}{g_i + \frac{t_d}{\varepsilon_r}}} \quad (4)$$

where t_d and ε_r are the thickness and the coefficient of the dielectric, respectively. Another important parameter in MEMS switches is the type of material used as a beam, which has a great effect on isolation and switching time.

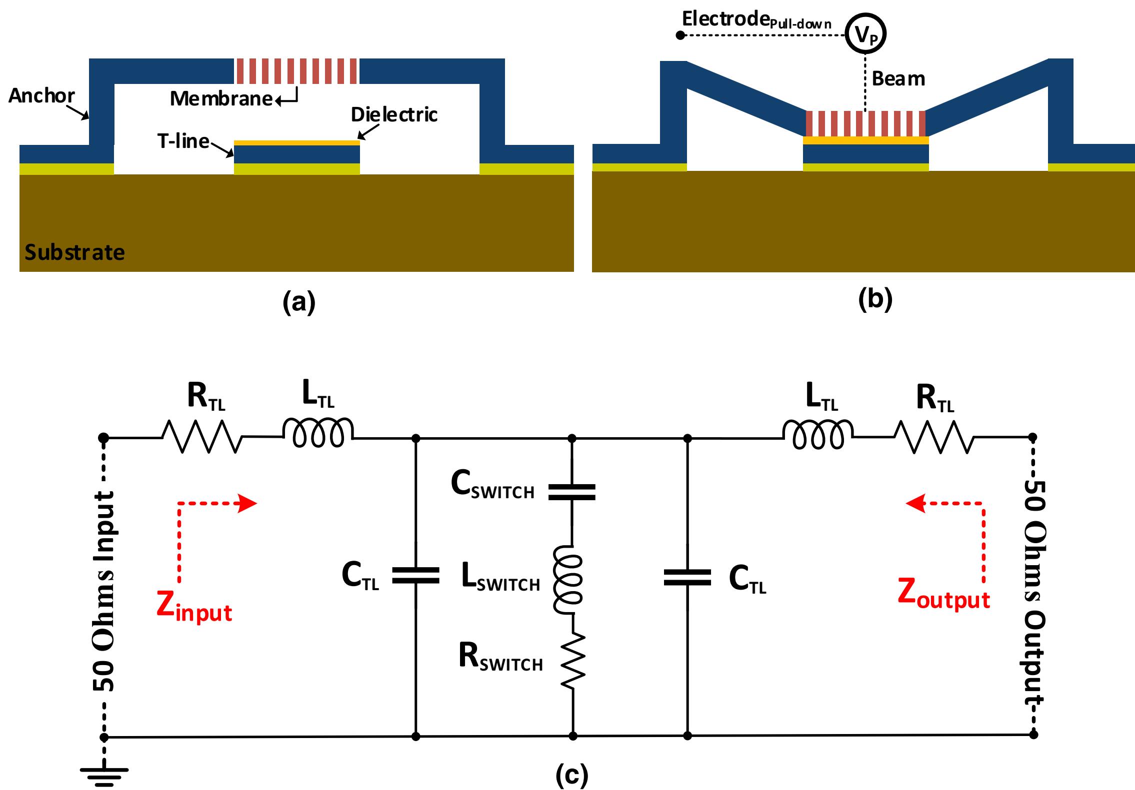

Fig. 1 Side view of the switch in (**a**) up state (off), (**b**) down state (on), (**c**) electrical model of the switch

The material used as a beam should have a high electrical conductivity to achieve good isolation. It also needs a small mass density to increase the resonance frequency according to Eq. (5). By increasing the resonance frequency, according to Eq. 6, the switching time will decreases and the switching speed increases.

$$\omega_0 = \sqrt{\frac{k}{m_{eff}}} \tag{5}$$

$$t_s = \frac{3.67 V_p}{V_s 2\pi f_0} \tag{6}$$

where ω_0 is the resonance frequency, k the spring-stiffness coefficient, m_{eff} the effective mass of the beam, t_s the switching time and $V_s = 1.4V_p$. The following equations can be used to obtain the Sparameter:

$$S_{11} = -20\log\left|\frac{-Z_h}{2Z_h + Z_0}\right| \tag{7}$$

$$S_{21} = -20\log\left|\frac{2Z_h}{2Z_h + Z_0}\right| \tag{8}$$

where Z_0 is the impedance of the CPW line and Z_h the impedance of the MEMS bridge.

3 Comparison of simulation and fabrication results

In this section, first three designed and fabricated switches in [10] are introduced. As shown in Fig. 2, three switches with different structures are fabricated by Shekhar et al. In Table 1, the results of the fabrication of the three switches are considered. As can be seen, these results are very suitable. In order to demonstrate the high credibility of the simulations, the same three switches are simulated and the results are compared with the results of the fabrication of these switches. As shown in Fig. 3, the results of the simulation are very close to the results of the fabrication, which indicates the credibility and high quality of the simulations.

4 Design and simulation of new switches

4.1 The main structure

To improve the results of the switches fabricated in [10], the original structure of the three switches was changed and three new switches were introduced using the new spring structure. As discussed in the previous section, the simulations presented in this paper are based on fabrication, and

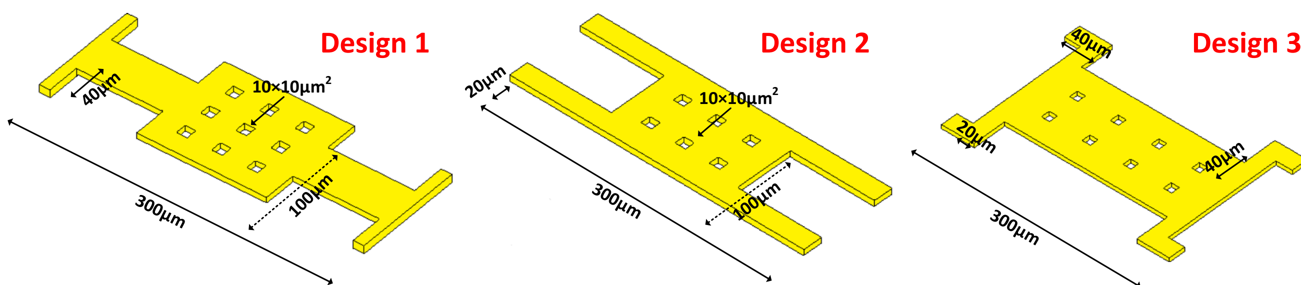

Fig. 2 Schematic of the three switches fabricated in [10]

Table 1 The results of the fabrication of the three switches presented in [10]

Parameter	Design 1	Design 2	Design 3
Actuation voltage (v)	5.4	6.3	4.8
Isolation	> 30 dB @ 17 GHz	> 40 dB @ 30 GHz	> 40 dB @ 40 GHz
Insertion loss	1 dB @ 20 GHz	< 0.25 dB @ 20 GHz	< 0.7 dB @ 40 GHz
Beam material	Au	Au	Au
Thickness (μm)	0.5	0.5	0.5
Switching time (μs)	12	14	18

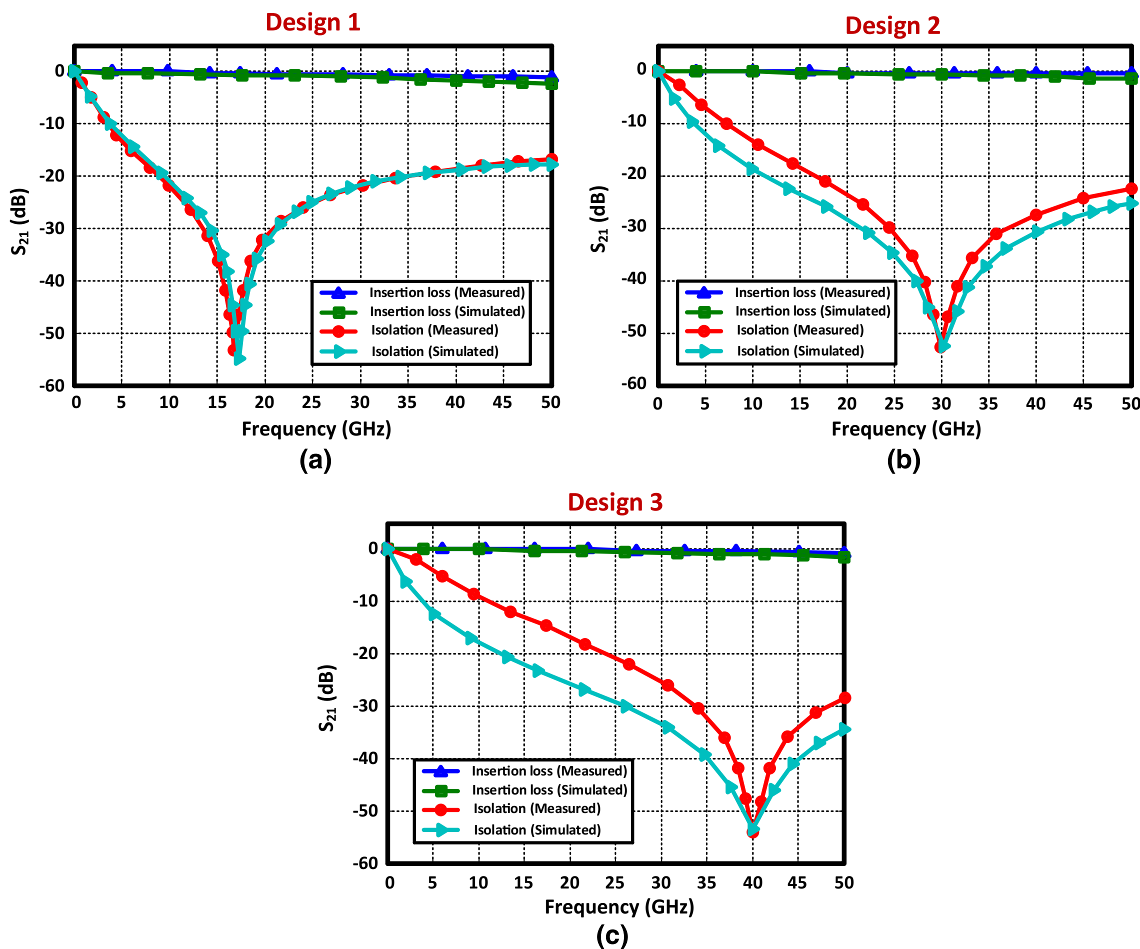

Fig. 3 Comparison of S-parameter for basic structures in fabrication and simulation (**a**) first structure (**b**) second structure (**c**) third structure

the same results will be obtained from simulations if three new switches are fabricated. Three new structures with their dimensions are shown in Fig. 4.

4.2 Effect of holes on the switch parameters

By placing several holes inside the membrane, the mass of the switch is reduced, which, according to Eq. 5, increases the resonance frequency, thereby reducing the switching time. In addition, after applying force when the beam is

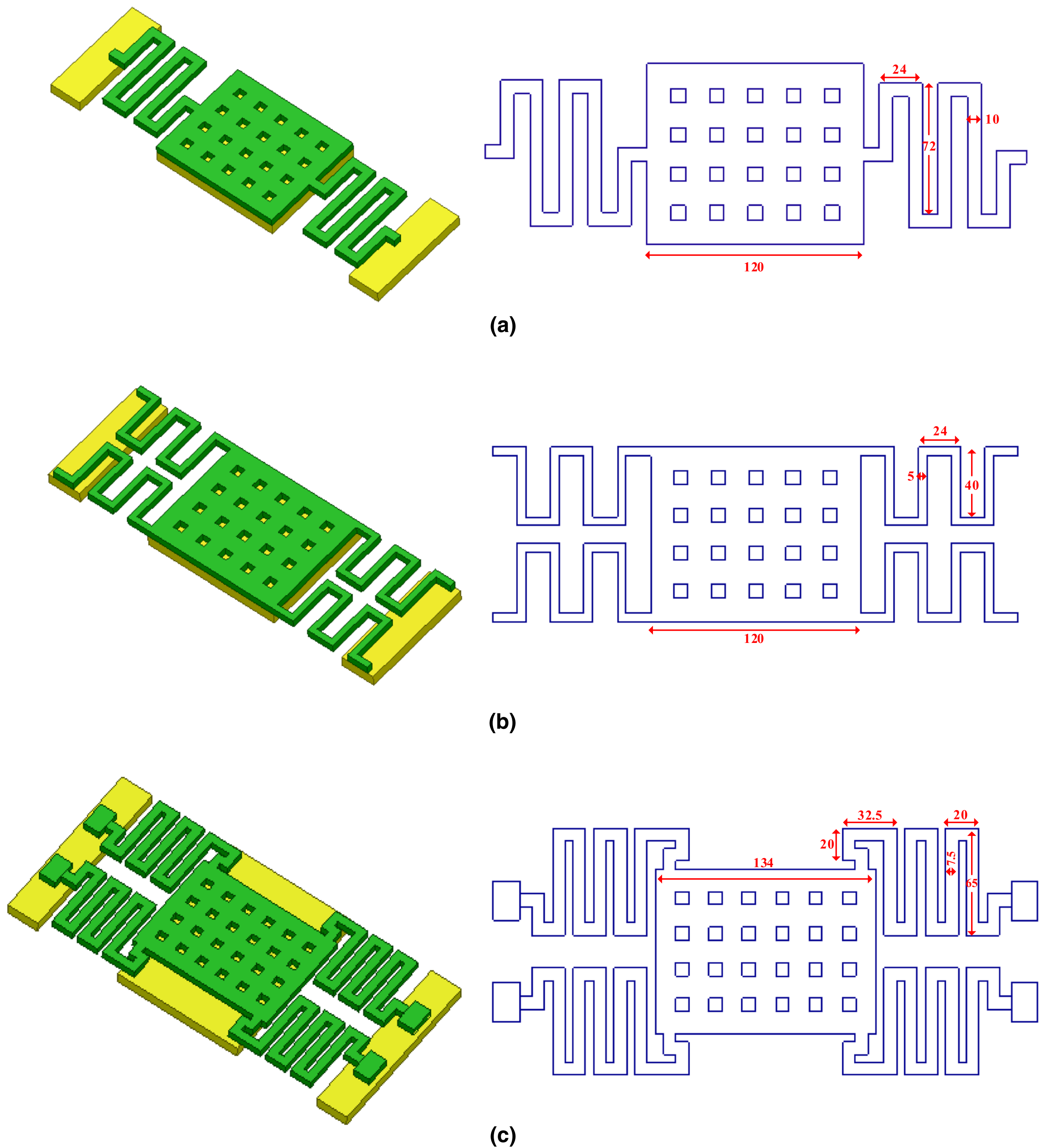

Fig. 4 Top view of three proposed switches with their dimensions (**a**) first design (**b**) second design (**c**) third design

pulled down, the air below holes goes out, which will make the pull-in and pull-up process easier to switch. But, there is a disadvantage in creating holes. By creating holes, the area of the cross-section of the switch decreases. As a result, the input signal is transmitted from the lower cross-section to the ground and the isolation decreases. To better understand this, one can refer to [3, 4].

4.3 The effect of changing the thickness of the beam on the switch

The switching time can be calculated using Eq. 6 and the releasing time can be evaluated using the following equation:

$$t_{pu} = \frac{1}{4f_0} = \frac{\pi}{2}\sqrt{\frac{m_{eff}}{k}} \tag{9}$$

where f_0 is the resonant frequency of the switch and t_{pu} the releasing time. The time that lasts the beam reaches the dielectric is t_s and the time duration that the beam returns to its original state is t_{pu}. Using the COMSOL software, the first three modes of resonance frequency for each structure are shown in Fig. 5. As seen, only the first mode matches with our expectation of the behavior of the MEMS switch. As a result, for three proposed switches, the resonant frequency is 21 kHz, 32 kHz and 26 kHz, respectively. In Table 2, the physical characteristics of the proposed switches are given. In addition, in Fig. 6, the releasing and switching times are compared for different beam thicknesses.

4.4 The actuation voltage and design of the spring structure

In Fig. 4, the spring structure of the designed three switches with their dimensions is seen. To obtain the spring-stiffness coefficient, we can use Eqs. 10 and 11:

$$K_{1,2,3\ldots} = \frac{EWt^3}{L^3} \tag{10}$$

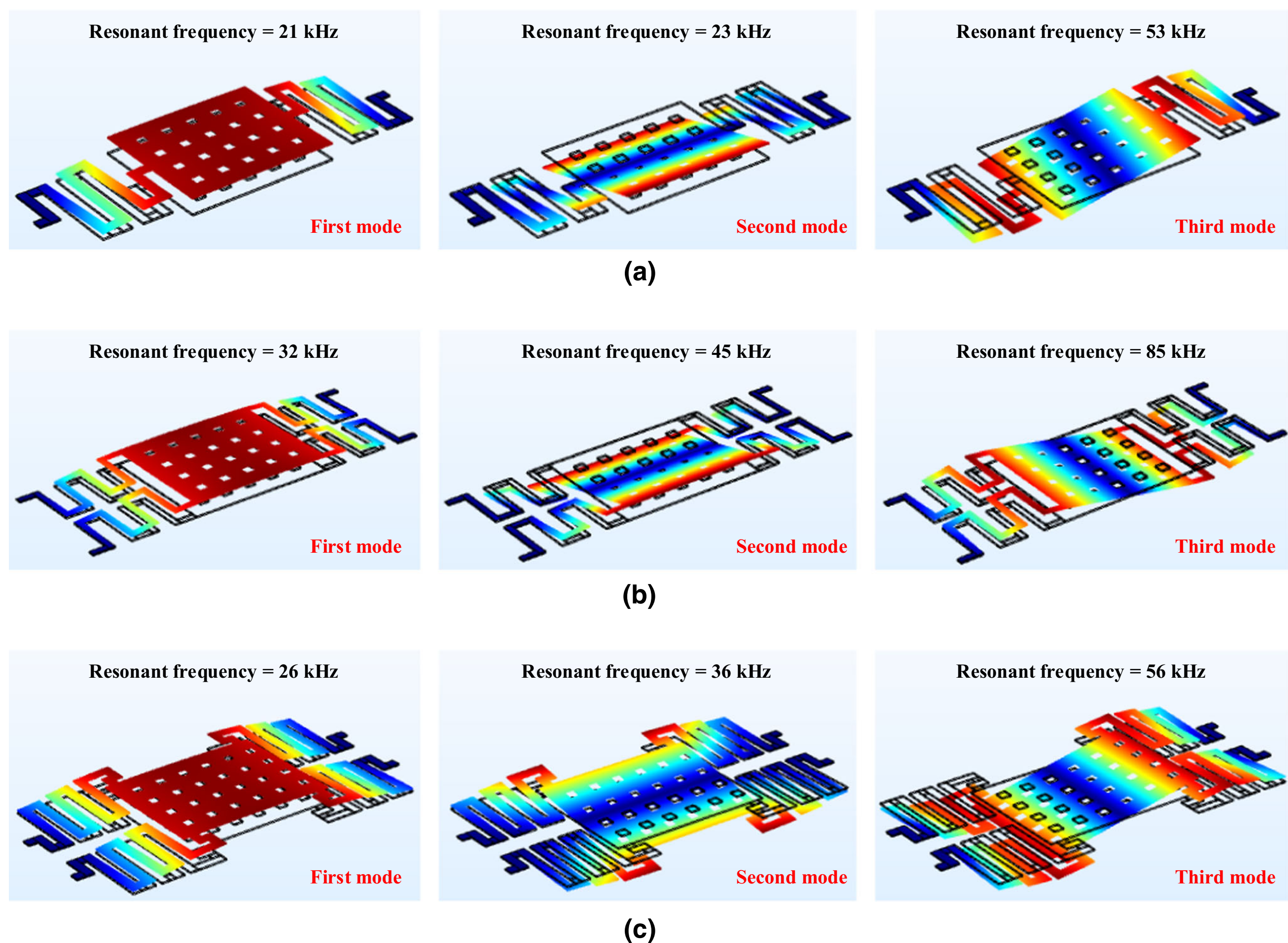

Fig. 5 The first three modes of the resonance frequency (**a**) first design (**b**) second design (**c**) third design

Table 2 Physical characteristics of the proposed Switches

Parameter	Design 1 (μm)	Design 2 (μm)	Design 3 (μm)
CPW dimensions	80/120/80		
CPW thickness	0.5		
Overlap area	100 × 120		
Bridge thickness	1.5		
Bridge dimensions	100 × 120		100 × 134
Hole dimensions	8 × 8		
Dielectric thickness	0.15		
Gap	1		

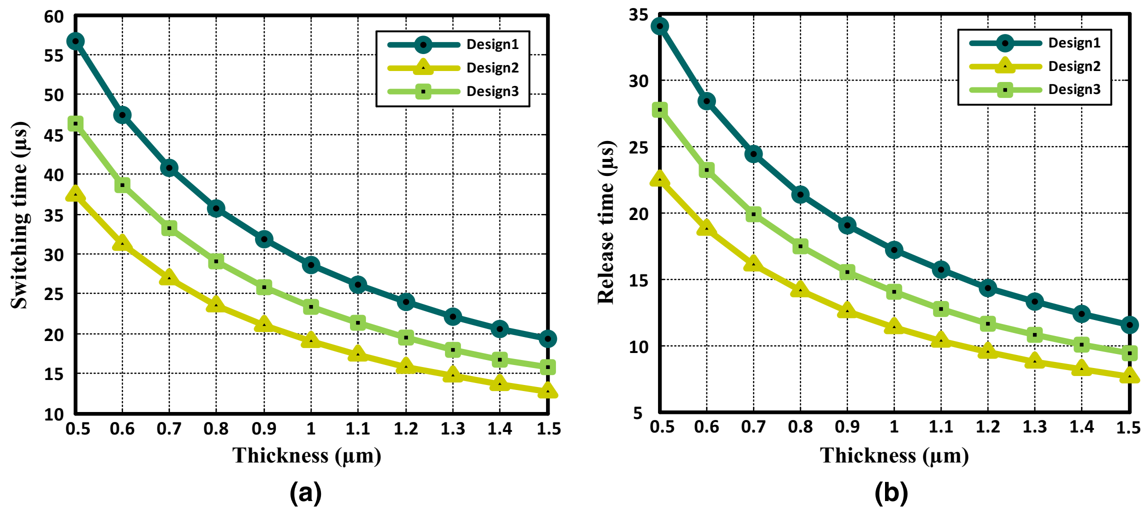

Fig. 6 Comparison of (**a**) the switching time and (**b**) the release time of the three proposed switches for different beam thicknesses

$$\frac{1}{K_x} = \frac{1}{K_1} + \frac{1}{K_2} + \frac{1}{K_3} + \cdots \quad (11)$$

where E is Young's modulus and W, t, and L the width, thickness, and length of each part of the spring, respectively. Given that in each of these structures four springs are used, according to Eq. 12, the stiffness coefficient of the total springs used in the switch is obtained as:

$$K_T = 4 \times K_x \quad (12)$$

4.5 Comparison of RF characteristics in Optimized Switches with Basic Switches

In the previous section, the optimization procedure of the switch using a new spring structure for each design was described. The switches fabricated in [10] uses Si_3N_4 as a dielectric layer. Simulations show that RF performance is improved by using a higher-coefficient of the dielectric. Therefore, in new designs, AlN is used as a dielectric layer, whose dielectric coefficient is higher than Si_3N_4, and it is also a hard material. Dielectric hardness is important due to the fact that it prevents the bulge and erosion in the high number of cycles during collision of the beam to the dielectric, which increases the lifetime of the switch. Figure 7 illustrates the isolation comparison for the proposed structures with the basic structures.

5 Results and discussion

The fabricated switches in [10] are optimized in four steps, which are discussed below:

5.1 Reduction of the actuation voltage

According to Eq. (1), there are three ways to reduce the actuation voltage: First way is to decrease g_i, the second way is to decrease K and the third one is to increase A, which is the best way to reduce the spring-stiffness coefficient [3, 4]. In this paper, three new structures for spring have been used to reduce the actuation voltage in a way that it reduces the stiffness of the spring. In addition, as far as possible, the gap between the beam and the dielectric has been reduced so that the self-actuation phenomenon and the degradation of the capacitive ratio do not occur.

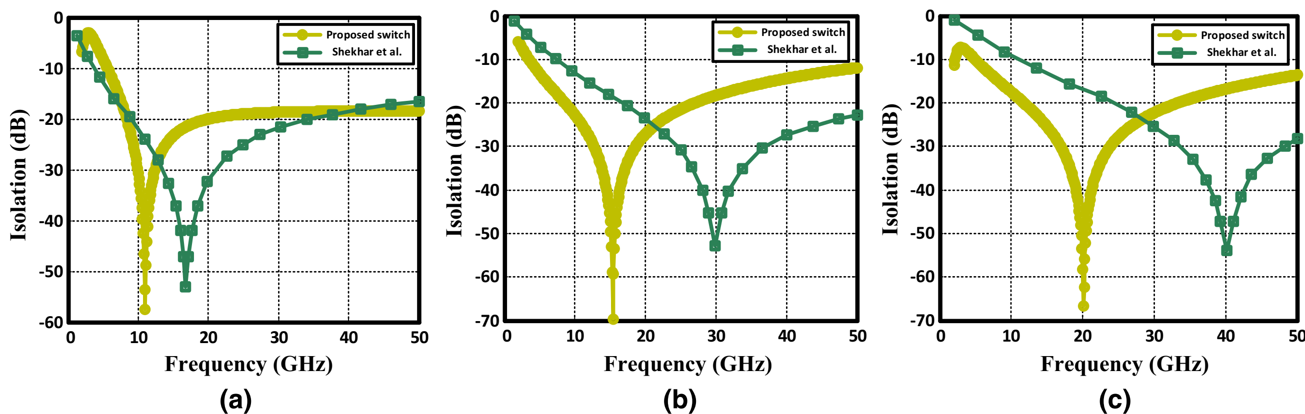

Fig. 7 Comparison of the isolation between the initial structures and the proposed structures (**a**) first design, (**b**) second design, (**c**) third design

Table 3 The results of the simulation of the three proposed switches

Parameter	Design 1	Design 2	Design 3
Actuation voltage (v)	2.4	5.9	3.5
Isolation	− 57 dB @ 11 GHz	− 65 dB @ 15 GHz	− 66 dB @ 20 GHz
Insertion loss	2 dB @ 11 GHz	0.3 dB @ 15 GHz	0.4 dB @ 20 GHz
Beam material	Al	Al	Al
Thickness (μm)	1.5	1.5	1.5
Switching time (μs)	19.3	12.7	15.7

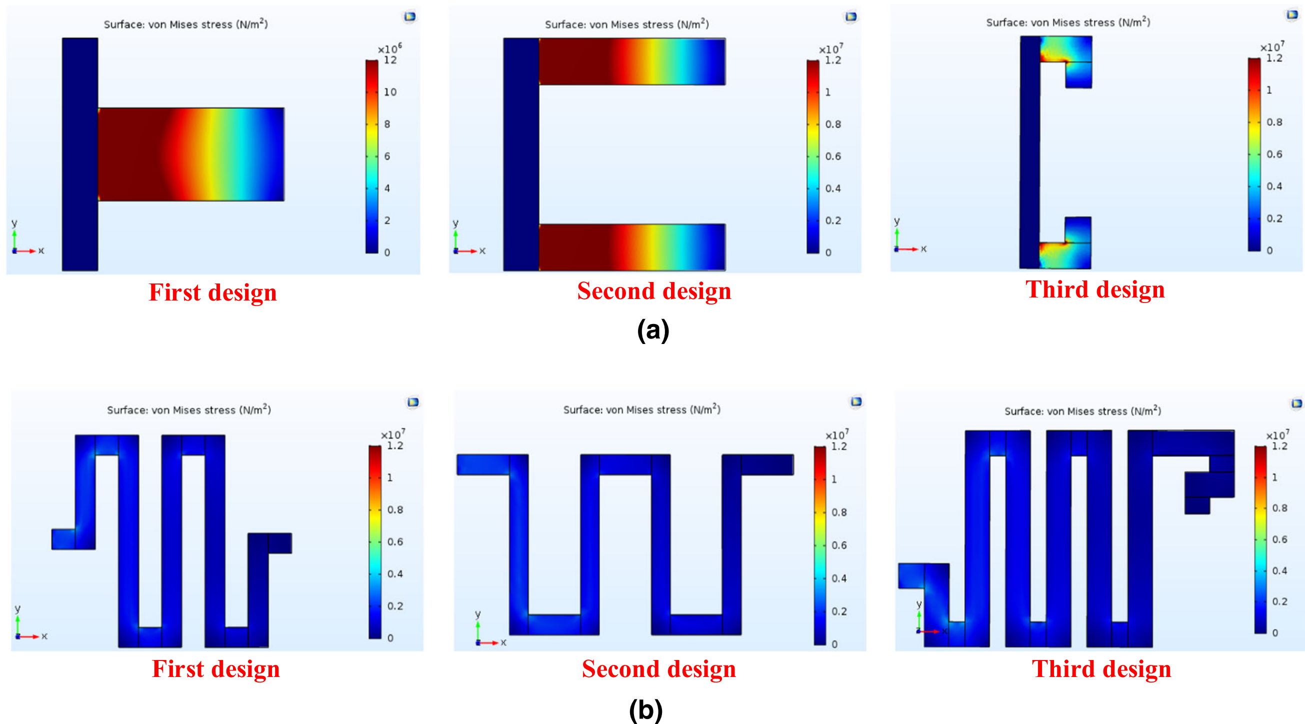

Fig. 8 Comparison of stress between (**a**) switches fabricated by Shekhar et al. [10]. **b** The proposed switches

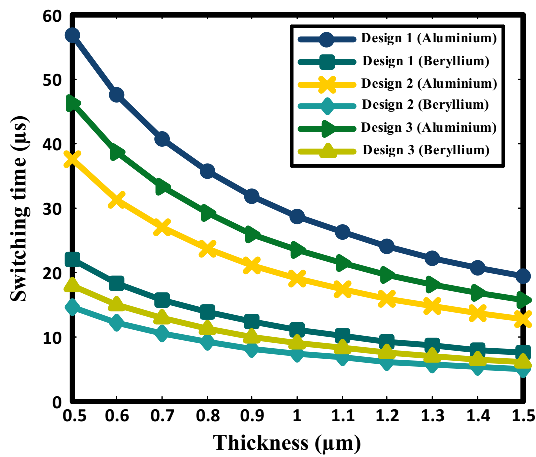

Fig. 9 Comparison of switching times for two materials of aluminum and beryllium in three proposed structures

5.2 Increase of the isolation

The choice of dielectric type is important for high isolation. In this paper, AlN has been used as a dielectric layer for all three structures, which has a high dialectic coefficient and it is considered a hard material, which results in a longer lifetime of the switch in a long time. Table 3 shows the value of the S-parameter and the actuation voltage for the new structures.

5.3 Reduction of the stress

After applying force to the beam, stress is applied to places where the springs are attached to the ground. This stress has a negative effect on the switch function and its lifetime in the high number of cycles. As shown in Fig. 8, the amount of stress applied to the switches fabricated by Shekhar et al. [10] is far greater than stress on the switches proposed in this

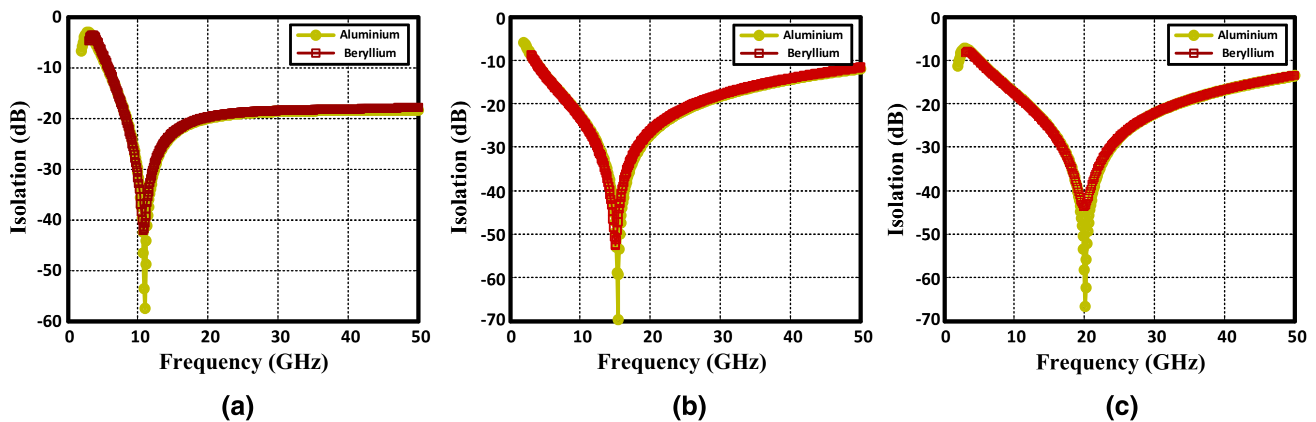

Fig. 10 Comparison of the isolation in the three proposed structures for the aluminum and beryllium switch

Table 4 Comparison of the proposed switches with previous work

Parameters	Ref. [3, 4]	Ref. [9]	Ref. [10]	Ref. [8]	This work
Actuation mechanism	Electrostatic	Electrostatic	Electrostatic	Electrostatic	Electrostatic
Switch beam material	Al	Al	Au	Au	Al
Thickness	0.5	1 µm	0.5 µm	2.2 µm	1.5 µm
Pull-in voltage	2.2 V	20 V	4.8–6.3 V	3.75–14.5 V	2.4–5.9 V
Return loss	− 11.47 dB @ 40 GHz	− 20 dB @ 24 GHz	–	–	− 11.47 dB @ 40 GHz
Insertion loss	− 0.65 dB @ 30.5 GHz	− 0.9 dB @ 24 GHz	− 0.25 dB @ 20 GHz; − 0.7 dB @ 520 GHz	0.005–0.06 dB @ 10 GHz	0.3–2 dB @ 11–20 GHz
Isolation	− 71 dB @ 30.5 GHz	− 18 dB @ 24 GHz	30–40 dB @ 17 GHz; 30 dB @ 40 GHz	70–76 dB @ 10 GHz	57–66 dB @ 11–20 GHz
Air gap	0.7; 1.8 and 2.8 µm	1 µm	2 µm	3 µm	1 µm

paper. To compare stress in these springs, a same force is applied to the point of attachment of the springs to the beam. Then, the stress range is considered between 0 and 12 MPa for all springs. This stress reduction is achieved using the designed spring structure in new switches.

5.4 Reduction of the switching time

As explained before, reduction of the switch mass can decrease the switching time. In this paper, the mass of the switch is reduced using a few holes inside the beam. But another way to reduce the mass of the switch is to use a substance with a mass less than aluminum. Beryllium is an excellent metal for the beam, because in addition to its low mass density, it has an electrical conductivity close to the aluminum, and in this way, it keeps the isolation of the switch in the desired range. To prove this claim, the switching times for the new structures using aluminum and beryllium are compared in Fig. 9. Also, Fig. 10 shows the isolation for new structures using these two materials. As it is seen, the switching time is significantly improved, which is an excellent advantage, and the isolation, although is reduced, is still excellent.

The switches designed in this article are compared with the previous works, the result of which is given in Table 4. It is clear that the results of this design are great compared to many previous works.

6 Conclusion

In this paper, the three basic structures were considered, and then, some important parameters of the switch including actuation voltage, switching time, stress and isolation are optimization in four steps. The lifetime of the switches was also increased by changing the type of Si_3N_4 to AlN, using a new spring structure. According to the results, actuation voltage and stress are reduced 50% and 65% after the completion of the optimization steps, respectively. Also, the isolation is increased by 16%.

References

1. Rebeiz, G. M. (2003). *RF MEMS: theory, design and technology* (3rd ed.). New Jersey: Wiley.
2. Rebeiz, G. M., et al. (2009). Tuning into RF MEMS. *IEEE Microwave Theory and Techniques Society, 10,* 55–72.
3. Ansari, H. R., & Khosroabadi, S. (2018). Design and simulation of a novel RF MEMS shunt capacitive switch with a unique spring for Ka-band application. *Microsystem Technologies, 25*(2), 531–540.
4. Ansari, H. R., & Khosroabadi, S. (2018). Low actuation voltage RF MEMS shunt capacitive switch with high capacitive ratio. In *Iranian conference on electrical engineering (ICEE).*
5. Khodadady, K., & Ganji, B. A. (2015). Design and modeling of a novel RF MEMS series switch with low actuation voltage. *Microsystem Technologies, 22*(12), 2921–2929.
6. Molaei, S., & Ganji, B. A. (2017). Design and simulation of a novel RF MEMS shunt capacitive switch with low actuation voltage and high isolation. *Microsystem Technologies, 23*(6), 1907–1912.
7. Mafinejad, Y., Kouzani, A. Z., Nassabi, M., Lim, Y., & Mafinezhad, K. (2015). Characterization and optimization to improve uneven surface on MEMS bridge fabrication. *Displays, 37,* 54–61.
8. Premila, L. S., & Naga, M. (2016). Optimization of structures of DC RF MEMS series switches for low actuation. *Microsystem Technologies, 23*(7), 2371–2379.
9. Mafinejad, Y., Kouzani, A., Mafinezhad, K., & Hosseinnezhad, R. (2017). Low insertion loss and high isolation capacitive RF MEMS switch with low pull-in voltage. *International Journal of Advanced Manufacturing Technology, 93,* 661–670.
10. Shekhar, S., Vinoy, K. J., & Ananthasuresh, G. K. (2017). Surface-micromachined capacitive RF switches with low actuation voltage and steady contact. *Journal of Microelectromechanical Systems, 26,* 643–652.
11. Cho, I., & Yoon, E. (2010). Design and fabrication of a single membrane push-pull SPDT RF MEMS switch operated by electromagnetic actuation and electrostatic hold. *Journal of Micromechanics and Microengineering, 20,* 035028.

Publisher's Note Springer Nature remains neutral with regard to jurisdictional claims in published maps and institutional affiliations.

Hamid Reza Ansari (born in 1994) received the B.Sc. degree in Electrical Engineering from Imam Reza International University, Mashhad, Iran, in 2016. He graduated from a Master degree in Mechatronics in 2018, at the same university. He is currently pursuing the Ph.D. degree in Nanoelectronics research domain with the Shiraz University of Technology, Shiraz, Iran. His research interests are MEMS modeling, Nanoelectronics, Hydrophones and RF MEMS switches.

Mojtaba Behnam Taghaddosi received the B.Sc. degree in Electrical Engineering from Shahid Bahonar University of Kerman (SBUK), Kerman, Iran, in 2000. He obtained his Masters in Control Engineering from Tarbiat Modares University, Tehran, Iran in 2004. After that he holds a Ph.D. in Mechatronics Engineering from Polytechnic University of Turin, Turin, Italy in 2011. He currently works as an assistant Professor in the Department of Electrical Engineering in Imam Reza International University. His main research interests and publications lie in the Semiconductor Devices, MEMS, Fuzzy Logic, and ABS brakes.